

Thermal properties of carbon nanotube array used for integrated circuit cooling

Yuan Xu, Yi Zhang,^{a)} and Ephraim Suhir

Nanoconduction Inc., 1275 Reamwood Avenue, Sunnyvale, California 94089

Xinwei Wang

Department of Mechanical Engineering, University of Nebraska-Lincoln, Lincoln, Nebraska 68588-0656

(Received 19 January 2006; accepted 24 July 2006; published online 4 October 2006)

Carbon nanotubes (CNTs), owing to their exceptionally high thermal conductivity, have a potential to be employed in micro- and optoelectronic devices for integrated circuit (IC) cooling. In this study we describe a photothermal metrology intended to evaluate the thermal conductivity of a vertically aligned CNT array (VCNTA) grown on a silicon (Si) substrate. Plasma-enhanced chemical vapor deposition, with nickel (Ni) as a catalyst, was used to grow CNT. The experimentally evaluated thermal conductivity of the VCNTA and the thermal contact resistance at the interface between the VCNTA and the “hot” surface was found to be in a satisfactory agreement with theoretical predictions. The measured effective thermal resistance is measured to be $0.12\sim 0.16\text{ cm}^2\cdot\text{K}/\text{W}$. This resistance was compared to the measured resistance of commercially available thermal grease. Based on this comparison, we conclude that, although the thermal resistance of CNTs might not be as low as it might be desirable, there exists a definite incentive for using VCNTA of the type in question for IC cooling. © 2006 American Institute of Physics. [DOI: [10.1063/1.2337254](https://doi.org/10.1063/1.2337254)]

I. INTRODUCTION

Carbon nanotubes (CNTs), since their discovery in 1991,¹ have attracted significant interest of a number of investigators. CNTs possess unique structure, as well as extraordinary mechanical, electrical, and optical properties.^{2–7} It has been shown that CNTs can be used as optoelectronic devices,^{8–10} field effect transistors (FETs),^{11–13} and sensors.^{14–17} It has been shown also that the thermal conductivity of CNTs can be exceptionally high, even higher than that of the diamond.¹⁸

Numerous studies, mostly theoretical, have been recently conducted to evaluate the thermal performance of CNTs and their applicability for heat removal in integrated circuit (IC) devices. Thermal conductivity of single wall carbon nanotubes (SWCNTs) was investigated using various simulation techniques, such as molecular dynamics (MD) simulation, nonequilibrium simulation and theory of force field.^{19–22} Although the obtained data are rather inconsistent and showed significant discrepancy, these data nonetheless confirmed that the expected level of CNT thermal conductivity could be quite high: 6000,¹⁹ 3750,²⁰ 1600,²¹ and 2980 W/m K,²² i.e., much higher than that of the majority of the known materials. There exists, therefore, a significant interest in using CNTs as thermal interface materials (TIMs) for thermal management of IC devices.

As to the experimental studies, it has been found²³ that the thermal conductivity of individual multiwall carbon nanotubes (MWCNTs) at room temperature could be as high as 3000 W/m K. This result is within the region of theoretical predictions. For SWCNT dense-packed ropes, however, a rather low value of 35 W/m K was obtained for mat-

samples.²⁴ Thermal conductivity level of 150 W/m K was reported by Shi *et al.*²⁵ for SWCNT in a bundle of CNT, with the average diameter (of a single CNT) of 10 nm. Theoretically, the thermal conductivity of MWCNT should be lower than the conductivity of the SWCNT ones, and, indeed, some experiments showed that the thermal conductivity of aligned MWCNT could be as low as 12–17 W/m K.²⁶ A somewhat higher value of 27 W/m K was obtained by several other research groups.^{27–29}

In general, the carried out investigations resulted in a reasonably satisfactory qualitative understanding of the thermal properties of CNTs. These investigations have indicated that the thermal conductivity of CNT bundles could be much lower than the theoretical predictions (1600–6600 W/m K) (Refs. 20–22) and the conductivity of single CNT.²³ There seemed to be several reasons for that.

First of all, the measurements show the results for an ensemble average, and there could be many “underperforming” (e.g., containing various flaws) individual CNTs in the tested samples. Second, there are typically CNT of different types and geometry in samples of large size and therefore it is simply impossible to “extract” information about the properties of a particular CNT type. The measured “effective” thermal conductivity is just an average number. Also, the uncertainty in the obtained information could be partially attributed to the inherently disordered nature of some CNTs grown by chemical vapor deposition (CVD). Most importantly, the boundary scattering of phonons could substantially reduce the thermal performance of CNTs. Finally, the thermal contact resistance between the CNTs and the heater could strongly affect the results of the measurements.

In any event, there is a clear indication that the CNT has a higher conductivity than the conductivity of regular TIM used today by the industry for IC cooling. The latter is only

^{a)}Electronic mail: yi@nanoconduction.com

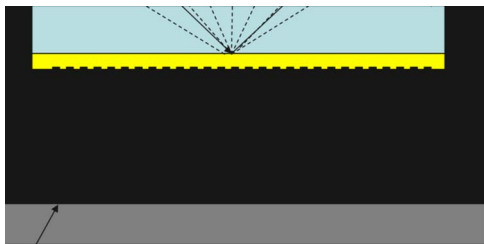


FIG. 1. (Color online) Sample assembling in experiment.

about 3–7 W/m K. It is clear also that the capabilities of thermal metrology, in terms of its accuracy and consistency, provide a significant challenge in our ability to correctly establish the “true” thermal conductivity of CNT arrays.

In this study, a photothermal experimental technique is developed with an objective to characterize, with the highest resolution possible, the thermal properties of the VCNTA designed to be used in the TIM capacity, i.e., to provide effective heat transport/removal from a “hot” surface. One of the main objectives of the developed technique is to develop a means that would enable one to distinguish between the thermal resistance of VCNTA and the interfacial thermal resistance at the boundary between the CNT and the hot surface (layer). For comparison and in order to establish whether there is sufficient incentive for using CNTs as heat removing means, we measured also, using the developed technique, the effective thermal resistance of commercially available grease that is currently used for thermal management of IC devices.

II. EXPERIMENTS

A. Principles

The samples used in our experiments (Fig. 1) are vertically aligned CNTs grown on a Si wafer (with Ni as the catalyst) by means of plasma-enhanced chemical vapor deposition (PECVD) in UNL. The samples are pressed against a Ni coated ZnSe window. The ZnSe material is chosen because of its transparency with respect to both the laser beam and the induced infrared (IR) radiation from the Ni film.

A pressure of 60 psi was applied to the back of the Si substrate to ensure good interfacial contact of the VCNTA with the Ni film. A modulated laser beam with the wavelength of 1.45 μm was focused onto the 100 nm thick Ni film, and the focal region was heated up. The assessed diameter of the laser focus spot was about 1 mm. The interfacial material (CNT) was expected to remove the major portion of the heat from the Ni film, owing to the low thermal resistance of this film. It is anticipated that the thermal conductivity of the interfacial material (CNTs) will have an appreciable and “measurable” effect on the thermal response of the Ni film to the modulated laser pulse, which affects the surface radiation of the Ni layer.

The phase shift signal is affected by the thermal properties of the interfacial material (CNT) in the test sample, while the delay in the phase is an indication on how fast the heat is transferred/removed from the heat source. The response to different frequencies is highly dependent, however,

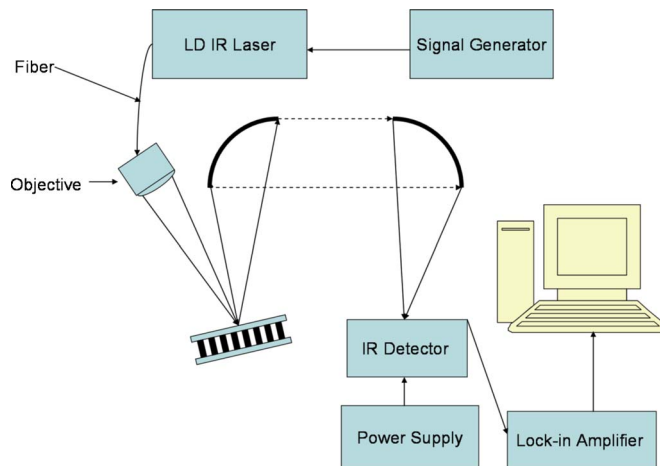


FIG. 2. (Color online) Experimental setup for measuring the total thermal resistance and thermal conductivity of the VCNTA.

on the level of the interfacial resistance and the thermal conductivity of the CNT array. In our study, we used the predictive model suggested by Wang *et al.*^{30–32} to calculate the thermophysical properties of materials from the measured phase shift signals. We measured these signals in a quite broad frequency region (2–100 KHz) and used the least squares difference as a suitable goodness-of-fit criterion to adjust the experimental data to the theoretical curves. Specifically, we established the governing parameters in the theoretical relationships based on the obtained experimental data and, based on this, evaluated the thermophysical properties of the VCNTA.

B. Experimental setup

The experimental setup that we used to measure the phase shift of the thermal radiation from the Ni film surface is shown in Fig. 2. The function generator sends a transistor-transistor logic signal to modulate the high power diode laser ($\lambda=1.45 \mu\text{m}$). A periodical laser pulse was triggered in our experiments at an average power of 1 W. This laser beam was focused onto the Ni film to generate a periodic heat source. The CNTs dissipate the heat away from the Ni film to the Si substrate. The thermal radiation from the Ni film was directed onto a pair of off-axis paraboloidal reflectors and collected by a liquid-nitrogen (N)-cooled IR detector. A germanium (Ge) window was placed in front of the detector to filter out the reflected laser beam. Therefore, only the IR signal from the Ni film was expected to be collected by the IR detector. The signal from the detector was finally measured by a lock-in amplifier. The phase shift signal was collected and averaged for different frequencies. High laser power amplified the signal-to-noise ratio. Such amplification is especially important for high frequencies, when the thermal radiation signal was low.

It should be pointed out that a portion of the measured phase shift should be attributed to the system itself. In order to exclude this portion and to obtain the most accurate information of the “absolute” phase shift, we carried out measurements, in which the Ge window was removed, so that the IR detector would be able to collect both the laser signals and

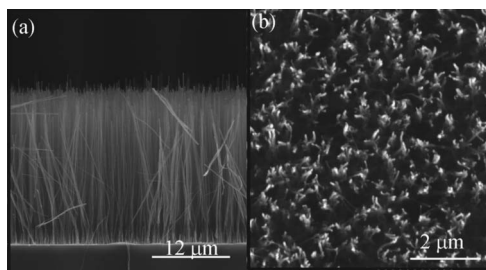


FIG. 3. Microscopic pictures for the CNT/CNF samples. (a) SEM cross section view of the CNT sample. (b) SEM top view of the CNT sample shows the high density of the CNT generated.

the IR signal. With a 1 W laser, the data for the amplitude, as indicated by the lock-in amplifier, have shown that the reflected laser signal was about 10^3 times greater than the IR signal. This means that the measured phase shift was dominated by the reflected laser signal. The final (“computed”) phase shift used for determination is $\theta_{\text{thermal}} - \theta_{\text{laser}}$, where θ_{thermal} is the phase shift measured for the thermal IR radiation from the Ni film, and the θ_{laser} is the phase shift due to the system itself on the basis of the reflected laser signal.

III. RESULTS AND DISCUSSION

The samples used in our experiments were manufactured (synthesized) using PECVD. The quality and the structure of the CNT samples could be judged based on the obtained scanning electron microscope (SEM) images (Fig. 3). The evaluated length of the CNT arrays was about $30 \mu\text{m}$ with a $3 \mu\text{m}$ variation. The assessed average diameter of the CNTs was about 100 nm, and the spacing between CNTs was also about 100 nm. The samples had a rather high CNT coverage density ($\sim 10^9$ CNT/cm²).

A. Calculated data

In our predictive modeling effort we used the model developed by Wang *et al.*^{30,31} (these authors used the photothermal method to study the thermal properties of multilayer thin film structure) and modified it to study the CNT properties treating the CNT array as, sort of, a composite material. The phase shift of the sample was measured in a broad frequency range (2–100 kHz) in order to obtain the most detailed information about the thermal conductivity and thermal interface resistance.

An example is provided in Fig. 4, which shows the relationship between the phase shift and the frequency for five different kinds of CNT materials. For all these materials, the interface contact resistance was set to $0.01 \text{ cm}^2 \text{ K/W}$, and the plotted curves represent the CNT material with total effective thermal resistances of 0.06, 0.11, 0.12, 0.15, 0.20, and $0.26 \text{ cm}^2 \text{ K/W}$, respectively. The assessed average length of the CNT samples was about $30 \mu\text{m}$.

The resolution of the experiment system and the calculation method was found to be high enough to distinguish between samples with an effective thermal resistance difference of $0.01 \text{ cm}^2 \text{ K/W}$. For instance, for samples with an effective thermal interfacial resistance of $0.01 \text{ cm}^2 \text{ K/W}$ and the total effective thermal resistances of 0.11 and

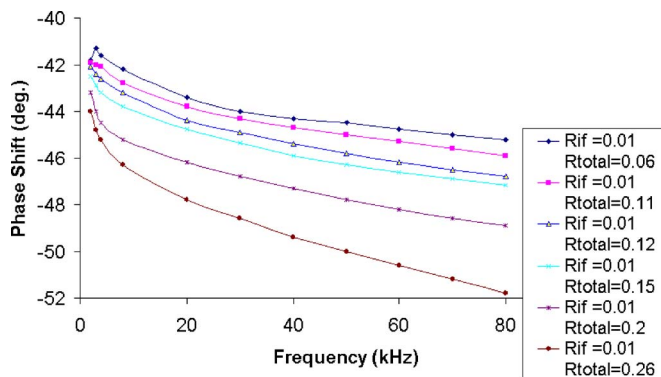


FIG. 4. (Color online) Calculated curves for the CNT material with a fixed interface thermal resistance and different total thermal resistances.

$0.12 \text{ cm}^2 \text{ K/W}$, the evaluated phase delay at 2000 Hz was 41.9° and 42.2° , respectively (Fig. 4). As a result of a long time observation of the phase delay signal at the frequency of 2000 Hz, it has been found that the variation of the signal is about 0.1° . This indicates that the resolution of the developed system is high enough to characterize the thermal performance of the CNT samples of the type in question. For higher frequencies, the phase delay difference between the above two samples becomes even more distinct, meaning that our experimental vehicle/setup is sensitive enough to characterize the thermal resistance of the CNT arrays of the addressed type.

B. Experimental results

The phase shift of the VCNTA and the data fitting curve are shown in Fig. 5. The calibrated phase shift of CNTs is obtained by subtracting the reference phase shift from the phase shift of the thermal radiation from the Ni film. The calibrated phase shift signal characterizes the thermal properties of the VCNTA sample. Based on the predictive model developed by Wang *et al.*,^{31,32} a four layer structure (ZnSe,

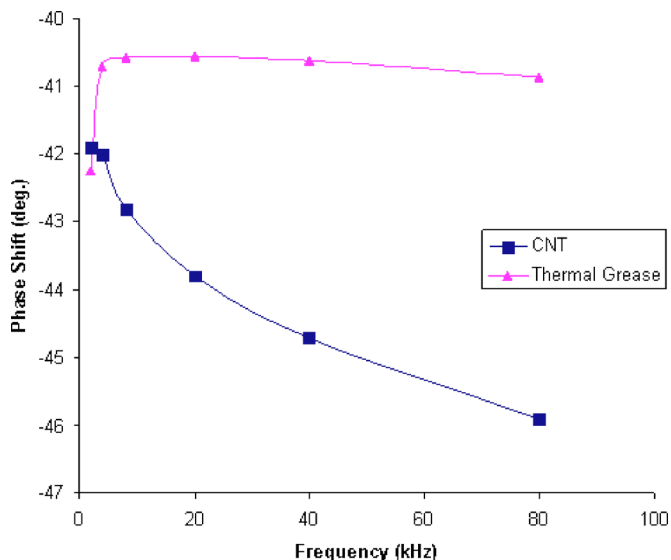


FIG. 5. (Color online) Fitted results of the CNT array calibrated phase shift measured from the thermal radiation from the Ni film. Thermal grease is also measured for comparison.

Ni film, CNTs, and Si substrate) was constructed and tested. The theoretical fitting curve matched well the measured phase shift curve in a wide range of frequencies. Only a 0.1° difference has been observed at the frequency range of 2–80 kHz.

The actual experimental results would be affected by some extrinsic parameters. On the other hand, according to our four-component structure setup, only the intrinsic properties of these layers would affect the final calculating results most. The thin Ni film (100 nm) has little effect on the measured phase shift due to the small thickness of the film. Therefore, the measured phase shift is dominated by the heat transfer from the Ni film to ZnSe and the Si substrate. The physical model used for data fitting considers all the heat transfer in the four components. In the experiment, the thickness and thermophysical properties of ZnSe, Ni, and Si are known. The only parameters that are unknown are the thermal contact resistance between Ni and CNT array, effective density of the CNT array, as well as its effective thermal conductivity. Theoretically, three sets of phase shift at different frequencies are sufficient to determine these three properties.³¹ In the experiment, the phase shift is measured over a wide frequency range. Different values of the unknown properties are used to calculate the theoretical phase shift and compare with the experimental result. The properties giving the best fit of the experimental data are taken as the properties of the CNT sample.

Based on the calibrated phase shift fitting and the employed physical model, the effective thermal conductivity and the effective density for the tested VCNTA sample were fitted to be 2.85 ± 0.05 K and 185 ± 1 kg/m³, respectively. The total effective thermal resistance of the sample could be calculated based on the information mentioned above $R = L/(k) = 0.12$ cm² K/W, where L ($30 \mu\text{m}$) is the length of the material in the heat transfer direction, K is the effective thermal conductivity, and A (1 mm^2) is the surface area. The thermal interface resistance between the CNT array and the Ni film was determined to be as low as 0.01 cm² K/W. Since the density of MWCNT is 2600 W/m K, the absolute thermal conductivity of the individual CNTs was calculated as $k = \rho / \rho_{\text{eff}} k_{\text{eff}} = 40.1$ W/m K. This relationship is physically reasonable because the thermal transport is only along the axial direction of CNTs in our experiment.

For verification/comparison purpose, commercially available thermal grease for IC cooling was also evaluated using the developed test vehicle. A thermal conductivity of 5.2 W/m K was obtained for this grease at room temperature. This result is consistent with the data provided by the manufacturer ($5 \sim 6$ W/m K). The evaluated thermal interface resistance was 0.02 ± 0.01 cm² K/W. This value is slightly higher than the one for the CNT sample that showed the total thermal resistance of 0.12 ± 0.01 cm² K/W for 2 mil ($50 \mu\text{m}$) thick thermal grease. These data confirm that the VCNTA thermal performance is attractive enough to consider such devices as an effective means for thermal managements of IC systems.

In our experiment, a load cell was put against a copper substrate to measure the forces applied on the CNT sample. The applied pressure was increased gradually, the corre-

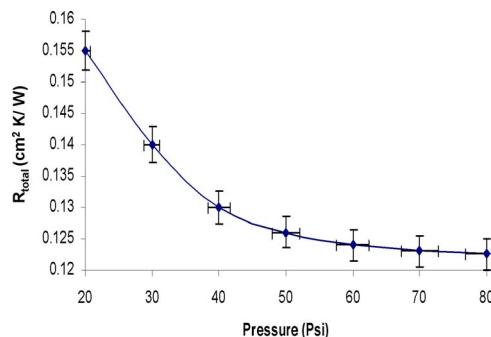


FIG. 6. (Color online) Relationship between the total thermal resistance of the CNTs and the applied pressure.

sponding phase delay of the CNT samples was concurrently measured, and the total effective thermal resistance was calculated as well. The results are shown in Fig. 6. For each point in this figure, the phase delay signal was acquired for the entire frequency region, and the corresponding thermal resistance was calculated. One can see that the total effective thermal resistance was reduced from 0.155 ± 0.01 cm² K/W to 0.12 cm² K/W and reached its steady-state value of about 0.12 ± 0.01 cm² K/W at the pressure of 80 psi. With a high pressure applied on the VCNT, it ensures that the thermal contact resistance between CNT arrays and the Ni film is much smaller than the effective thermal resistance of the CNTs themselves. As a result, the heat transfer from the Ni film to the Si substrate is mostly affected by the CNT array and makes it possible to measure the thermophysical properties of CNT arrays. If no pressure or low pressure is applied on the ZnSe, the CNT array will have poor contact with the Ni film, in other words, less number of CNTs would be in contact with Ni film, leading to a large thermal contact resistance between CNT arrays and the Ni film.

C. Discussion

The obtained experimental results have indicated that the VCNTA sample had a thermal conductivity of about 40.1 W/m K, and a total thermal resistance between $0.12 \sim 0.16$ cm² K/W. This level of thermal performance is competitive with the currently used commercial thermal interface materials. However, the measured thermal conductivity of the VCNTA was far below the values predicted by most of the research reported in the literature. There is a reason to believe that one of the major causes of such a deviation is

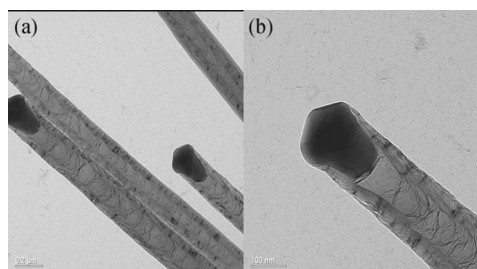


FIG. 7. HRTEM picture indicates the detail structure of the CNT sample (a) the “bamboo” structure of the CNTs, (b) enlarged view of the detailed structure of CNTs’ Ni top.

that in the measured CNTs a disordered amorphous carbon structure was present. The amorphous carbon layer surrounds the graphite layer structure of the CNTs as one could see in Fig. 7 (on top of the CNT array). This layer is acting as an undesirable isolator and prevents the VCNTA from having good contact with the Ni film, thereby preventing heat from being transferred into the graphitic layer.

Another possible reasons for a not-very-high thermal conductivity of the CNT array systems are the defects/flaws in the CNT structure. Transmission electron microscope (TEM) images (Fig. 7) showed that the CNT sample had a large number of defects and a “bamboo-type” structure. This causes significant phonon scattering in the material, thereby leading to a much reduced thermal conductivity.

IV. CONCLUSION

The following conclusions could be drawn from the performed analysis. (1) A photothermal metrology has been developed to characterize the thermal transport in VCNTA. (2) The thermal conductivity of the CNT arrays and the thermal contact resistance between the CNT and the heated Ni film was evaluated with a rather high accuracy using the developed test vehicle. (3) Based on the conducted experiments, we conclude that there exists a definite incentive for using VCNTAs for IC cooling. (4) The TEM and SEM observations have shown the possibilities for considerably improving the thermal performance of the existing structures by optimizing the CNT growth conditions and possibly by considering some specially designed postprocessing means to remove the amorphous carbon.

ACKNOWLEDGMENTS

One of the authors (X.W.) gratefully acknowledges the support from NSF (CTS: 0400458) and Layman Award of the University of Nebraska-Lincoln.

¹S. Iijima and T. Ichihashi, *Nature (London)* **363**, 603 (1993).

²M. S. Dresselhaus, G. Dresselhaus, and Ph. Avouris, *Carbon Nanotubes,*

Synthesis, Structure, Properties, and Applications (Springer, New York, 2000).

³R. H. Baughman, A. A. Zakhidov, and W. A. de Heer, *Science* **297**, 787 (2002).

⁴E. W. Wong, P. E. Sheehan, and C. M. Lieber, *Science* **277**, 1971 (1997).

⁵M. F. Yu, B. S. Files, S. Arepalli, and R. S. Ruoff, *Phys. Rev. Lett.* **84**, 5552 (2000).

⁶T. W. Odom, J. L. Huang, P. Kim, and C. M. Lieber, *Nature (London)* **391**, 62 (1998).

⁷J. W. G. Wilder, L. C. Venema, A. G. Rinzler, R. E. Smalley, and C. Dekker, *Nature (London)* **391**, 59 (1998).

⁸J. Li, Q. Ye, A. Cassell, H. T. Ng, R. Stevens, J. Han, and M. Meyyappan, *Appl. Phys. Lett.* **82**, 2491 (2003).

⁹R. H. Baughman *et al.*, *Science* **284**, 1340 (1999).

¹⁰A. Star, Y. Lu, K. Bradley, and G. Gruner, *Nano Lett.* **4**, 1587 (2004).

¹¹S. J. Tan, A. R. M. Verschuere, and C. Dekker, *Nature (London)* **393**, 49 (1998).

¹²P. C. Collins, M. S. Arnold, and P. Avouris, *Science* **292**, 706 (2001).

¹³A. Bachtold, P. Hadley, T. Nakanishi, and C. Dekker, *Science* **294**, 1317 (2001).

¹⁴J. Koehne, H. Chen, J. Li, A. Cassell, Q. Ye, H. T. Ng, J. Han, and M. Meyyappan, *Nanotechnology* **14**, 1239 (2003).

¹⁵J. Kong, N. R. Franklin, C. Zhou, M. G. Chapline, S. Peng, K. Cho, and H. Dai, *Science* **287**, 622 (2000).

¹⁶J. Li, Y. Lu, Q. Ye, M. Cinke, J. Han, and M. Meyyappan, *Nano Lett.* **3**, 929 (2003).

¹⁷J. P. Novak, E. S. Snow, E. J. Houser, D. Park, J. L. Stepnowski, and R. A. McGill, *Appl. Phys. Lett.* **83**, 4026 (2003).

¹⁸R. S. Ruoff and D. C. Lorents, *Carbon* **33**, 925 (1995).

¹⁹S. Berber, Y. Kwon, and D. Tománek, *Phys. Rev. Lett.* **84**, 4613 (2000).

²⁰S. Maruyama, *Microscale Thermophys. Eng.* **7**, 41 (2003).

²¹M. A. Osman and D. Srivastava, *Nanotechnology* **12**, 21 (2001).

²²J. Che, T. Çağın, and W. A. Goddard III, *Nanotechnology* **11**, 65 (2000).

²³P. Kim, L. Shi, A. Majumdar, and P. L. McEuen, *Phys. Rev. Lett.* **87**, 215502 (2001).

²⁴J. Hone, B. Batlogg, Z. Benes, A. T. Johnson, and J. E. Fischer, *Science* **289**, 1730 (2000).

²⁵L. Shi, D. Li, C. Yu, W. Jang, D. Kim, Z. Yao, P. Kim, and A. Majumdar, *J. Heat Transfer* **125**, 881 (2003).

²⁶D. J. Yang *et al.*, *Phys. Rev. B* **66**, 165440 (2002).

²⁷W. Yi, L. Lu, Z. Dian-lin, Z. W. Pan, and S. S. Xie, *Phys. Rev. B* **59**, R9015 (1999).

²⁸S. Xie, W. Li, Z. Pan, B. Chang, and L. Sun, *J. Phys. Chem. Solids* **61**, 1153 (2000).

²⁹L. Lu, W. Yi, and D. L. Zhang, *Rev. Sci. Instrum.* **72**, 2996 (2001).

³⁰X. W. Wang, Z. Zhong, and J. Xu, *J. Appl. Phys.* **97**, 064302 (2005).

³¹X. W. Wang, H. Hu, and X. Xu, *J. Heat Transfer* **123**, 138 (2001).

³²H. Hu, X. W. Wang, and X. Xu, *J. Appl. Phys.* **86**, 3953 (1999).